sustainability

MDPI

Article

Recovery of Valuable Metals from Spent $LiNi_{0.8}Co_{0.1}Mn_{0.1}O_2$ Cathode Materials Using Compound Leaching Agents of Sulfuric Acid and Oxalic Acid

Chunyuan Yang [1,2,†], Jiawei Wang [1,2,3,†], Pan Yang [1,2], Yue He [1,2], Song Wang [1,2], Pingyuan Zhao [1,2] and Haifeng Wang [1,2,3,*]

1 College of Materials and Metallurgy, Guizhou University, Guiyang 550025, China
2 Guizhou Provincial Key Laboratory of Metallurgical Engineering and Energy Saving, Guiyang 550025, China
3 Guizhou Provincial Engineering Technology Research Center of Manganese Materials for Batteries, Tongren 554300, China
* Correspondence: mm.hfwang@163.com
† These authors contributed equally to this work.

Abstract: The recovery of valuable metals from spent lithium-ion batteries is beneficial to protect the environment and avoid resource depletion. Based on the synergistic effect of the reducing ability of oxalic acid and the acidic strength of sulfuric acid, this study was conducted to recover valuable metals from spent $LiNi_{0.8}Co_{0.1}Mn_{0.1}O_2$ lithium-ion battery cathode materials with the compound leaching agents of sulfuric acid and oxalic acid. Under the optimized conditions of sulfuric acid concentration at 2.5 mol·L^{-1}, oxalic acid concentration at 20 g·L^{-1}, liquid-to-solid ratio at 10 mL·g^{-1}, reaction temperature at 85 °C, and reaction time at 100 min, the leaching rate of Li, Ni, Co, and Mn measured by ICP-OES was, respectively, 99.26%, 98.41%, 96.95%, and 97.54%. It was further validated that the valuable metals were almost completely leached when combined with the XRD and SEM-EDS analysis of spent cathode materials before and after leaching. The leaching of Li, Ni, Co, and Mn was all in accordance with the Avrami model with their activation energies of 31.96 kJ·mol^{-1}, 41.01 kJ·mol^{-1}, 47.57 kJ·mol^{-1}, and 42.95 kJ·mol^{-1}, indicating that the diffusion was the control of the Li leaching process, and the surface chemical reaction was the control of the other three metals. This work provides a new idea and method for the recycling of spent lithium-ion batteries.

Keywords: spent NCM ternary lithium-ion battery; sulfuric acid; oxalic acid; leaching rate; leaching kinetics

check for updates

Citation: Yang, C.; Wang, J.; Yang, P.; He, Y.; Wang, S.; Zhao, P.; Wang, H. Recovery of Valuable Metals from Spent $LiNi_{0.8}Co_{0.1}Mn_{0.1}O_2$ Cathode Materials Using Compound Leaching Agents of Sulfuric Acid and Oxalic Acid. *Sustainability* **2022**, *14*, 14169. https://doi.org/10.3390/su142114169

Academic Editors: Alessandra Zanoletti, Elsayed Mousa and Guozhu Ye

Received: 27 September 2022
Accepted: 24 October 2022
Published: 30 October 2022

Publisher's Note: MDPI stays neutral with regard to jurisdictional claims in published maps and institutional affiliations.

Copyright: © 2022 by the authors. Licensee MDPI, Basel, Switzerland. This article is an open access article distributed under the terms and conditions of the Creative Commons Attribution (CC BY) license (https://creativecommons.org/licenses/by/4.0/).

1. Introduction

Lithium-ion batteries are widely used in portable electronics, aerospace, medical devices, and other fields for their high specific capacity, good cycling performance, small self-discharge, and no memory effect [1,2]. As lithium-ion batteries begin to be used in large quantities in the field of new energy vehicles, there will be an explosive increase in the production and use of lithium-ion power batteries [3,4]. At present, commercial lithium-ion battery cathode materials are: $LiCoO_2$(LCO), $LiMn_2O_4$(LMO), $LiFePO_4$ (LFP), $LiCo_xNi_yMn_zO_2$ (NCM), etc. [5,6]. With the advantages of high energy density, low-temperature resistance, and low cost, the NCM ternary material has become the pioneer of lithium-ion battery cathode materials and occupied a dominant position in the market [7]. The service life of lithium-ion batteries as consumables is about 3–5 years, and the global amount of spent NCM ternary lithium-ion batteries has reached 300,000 tons in 2020, and the amount is expected to reach 720,000 tons by 2023 [8,9]. The spent ternary batteries contain toxic nickel, cobalt, manganese, and other metal components, which cause serious pollution to the environment if they are not properly treated [10]. At the same time, the

abundance of metal resources from spent ternary lithium-ion batteries is much greater than natural mineral reserves, which can be regarded as prosperous "city mines" [11]. Rational treatment of spent lithium-ion batteries and recycling of valuable metals can not only avoid environmental pollution caused by spent batteries, but also broaden the sources of scarce resources such as nickel, cobalt, and manganese [12]. This is of great significance for promoting the healthy development of the lithium-ion battery industry.

The recovery methods of valuable metals from cathode materials of spent lithium-ion batteries are mainly divided into the following three types: pyrometallurgy, hydrometallurgy, and biological metallurgy [13]. Pyrometallurgy refers to the process of enriching valuable metals in the form of alloys or metal compounds by high-temperature treatment [14]. The biggest advantage of pyrometallurgy is that it can process various types of spent lithium-ion batteries. The process is simple and easy to operate, and the technical process is relatively mature. However, high-temperature treatment not only consumes a lot of energy, but also produces a large amount of SO_2 and other toxic waste gases during the smelting process, causing serious environmental pollution [15]. Biological metallurgy is a technology that utilizes the oxidation and reduction characteristics of microorganisms in life activities to separate metals from the original material in the form of ions or precipitations in aqueous solutions [16]. Biological metallurgy is an environmentally friendly metal recovery method with mild reaction conditions and low economic input. However, biological metallurgy also has its fatal shortcomings: a long breeding cycle of strains, slow leaching reaction speed, and high time cost. It is difficult to meet the market demand for spent lithium-ion battery processing capacity, which limits its large-scale practical application in industrial production. Compared with the previous two methods, hydrometallurgy has incomparable advantages such as high comprehensive metal recovery, low energy consumption, environmental protection, and easier automation and continuity in the production process [17]. Therefore, hydrometallurgy is the most widely used method for recovering valuable metals from spent lithium-ion battery cathode materials [18].

The leaching process of valuable metals is a very important step in the whole recycling process from spent lithium-ion batteries. A brief summary of metal recovery from spent LIBs by different leaching systems is shown in Table 1. H_2SO_4 [19], HCl [20], HNO_3 [21], and other inorganic acids are first used for leaching, since the cathode material contains high-valence cobalt, manganese, and other metal ions that are insoluble in water, it is necessary to cooperate with H_2O_2 or other reducing agents to reduce them to a low-valent state [22]. Although it can achieve a high metal leaching rate, it also has some disadvantages such as the strong corrosiveness of the leaching agent and the generation of toxic and harmful gases during the leaching process [23]. Therefore, more environmentally friendly organic acids (citric acid [24], lactic acid [25], glucose acid [26], etc.) are beginning to be used to recover valuable metals. However, the acidity of organic acid is weak, and the H+ ion cannot be completely ionized. Only using organic acid for leaching will consume a large amount of expensive organic acid, high temperature, large liquid-to-solid ratio, and other conditions are often required to strengthen the leaching, and the cost will therefore increase furthermore [27].

Herein, the strategy of using compound leaching agents of inorganic acid and organic acid to recover valuable metal elements from spent lithium-ion battery cathode materials is proposed in this paper. Sulfuric acid is considered the most efficient and cheapest leaching agent [28]. Oxalic acid is a natural organic acid that is widely found in spinach, beet, and other plants. In the process of leaching the cathode material of spent lithium-ion batteries, oxalic acid can be used as both a leaching agent and a reducing agent [29]. This is because oxalic acid is a kind of strong acid in organic acids, which can ionize part of the H^+ ion. At the same time, it has a strong reducing property, so it can reduce high-valence metal ions to low-valence states and improve the leaching rate of metals [30]. Based on the synergistic effect of the reducing ability of oxalic acid and the acidic strength of sulfuric acid [31], the researchers used the compound leaching agents of sulfuric acid and oxalic acid to recover tin from hazardous zinc-leaching residue and indium from indium-bearing zinc

ferrite, which achieved a good effect [31,32]. By reviewing the relevant literature, there is no relevant report on the recovery of spent NCM ternary lithium-ion battery cathode materials. Therefore, the compound leaching agents of sulfuric acid and oxalic acid are the first to recover valuable metals from the cathode materials of NCM ternary lithium-ion batteries. The H^+ ionized by environmentally friendly oxalic acid can enhance the acidity of the solution and reduce the amount of cheap sulfuric acid. At the same time, oxalate can reduce the high-valence cobalt and manganese elements. This method has the advantages of less environmental pollution and low production cost. The effects of sulfuric acid concentration, oxalic acid concentration, liquid-to-solid ratio, reaction temperature, and reaction time on the leaching rate of valuable metal from the cathode materials of spent ternary lithium-ion battery were investigated by single factor experiment, and the optimal conditions for recovering valuable metals were obtained. In addition, the unreacted shrinking core model and Avrami model were used to study the leaching kinetics of spent ternary lithium-ion battery cathode materials to better understand the mechanism of the leaching process.

Table 1. A brief summary of metal recovery from spent LIBs by different leaching systems.

Cathode Material	Acid	Reductant	Other Leaching Conditions	Leaching Efficiency	Cost ($)	Ref.
NCM	H_2SO_4 = 2.5 mol·L^{-1}	oxalic acid = 20 g·L^{-1}	temperature = 85 °C, time = 100 min, S/L 10 g·L^{-1}	99.26% Li, 98.41% Ni, 96.95% Co, 97.54% Mn	3.14	This work
NCM	H_2SO_4 = 2.5 mol·L^{-1}	H_2O_2 = 2 vol %	temperature = 85 °C, time = 2 h, S/L ratio = 5 g·L^{-1}	Nearly 100% Li, 98% Ni, 97% Co, 96% Mn	46.69	[19]
NCM	HCl = 6 mol·L^{-1}	H_2O_2 = 5 vol %	temperature = 85 °C, time = 2 h, S/L ratio = 12.5 g·L^{-1}	99% Li, 98% Ni, 97% Co, 98% Mn	59.12	[20]
NCM523	HNO_3 = 0.5 mol·L^{-1}	$C_6H_8O_6$ = 0.5 mol·L^{-1}	temperature = 85 °C, time = 10 min, S/L ratio = 20 g·L^{-1}	nearly 100%, Li, Ni, Co, and Mn	37.21	[21]
NCM111	$C_6H_8O_7$ = 2.0 mol·L^{-1}	H_2O_2 = 2 vol %	temperature = 80 °C, time = 90 min, S/L ratio = 30 g·L^{-1}	99% Li, 97% Ni, 95% Co, 94% Mn	45.33	[22]
NCM	$C_3H_6O_3$ = 1.5 mol·L^{-1}	H_2O_2 = 0.5 vol %	temperature = 70 °C, time = 20 min, S/L ratio = 20 g·L^{-1}	97.7% Li, 98.2% Ni, 98.8% Co, 98.4% Mn	1.8×10^4	[23]
NCM111	$C_6H_{12}O_7$ = 1.0 mol·L^{-1}	H_2O_2 = 1 mol·L^{-1}	temperature = 70 °C, time = 80 min, S/L ratio = 30 g·L^{-1}	99% Li, 99% Ni, 97% Co, 96% Mn	9.1×10^6	[24]
NCM622	H_2SO_4 = 1.8 mol·L^{-1}	ginkgo biloba = 9 g·L^{-1}	temperature = 80 °C, time = 40 min, S/L ratio = 15 g·L^{-1}	99.99 % Li, 98.65% Ni, 98.41 % Co, 98.25% Mn	64.8	[25]

2. Experimental Section

2.1. Materials and Reagents

The spent NCM ternary lithium-ion battery cathode material used in the experiments is a sample provided by a company in Guizhou (the proportion of nickel, cobalt, and manganese was unknown). The nitric acid, hydrochloric acid, sulfuric acid, oxalic acid, and other reagents were all analytical grade and from Shanghai Macklin, Biochemical Technology Co., Ltd. (Shanghai, China). Additionally, the solvent of the solution used was pure water.

2.2. Experimental Procedure

An amount of 0.2 g of lithium-ion battery cathode powder was added to 40 mL aqua regia solution (HNO_3:HCl = 1:3, *v/v*), and digested to nearly dry at 80 °C, the solution after filtration was diluted with pure water to constant volume, and the concentration of each metal element was measured by ICP-OES, to determine the content of the valuable metal in the sample.

A certain volume of sulfuric acid and the oxalic acid solution was put into a three-neck flask with a condenser, and the flask was under a thermostatic water bath. When the temperature rose to the set temperature, 100 g of spent battery cathode powder was added to the flask, and the stirrer started to work at the speed of 500 RMP. The content of Li, Ni, Co, and Mn in the leaching solution was determined by ICP-OES, and the leaching rate of each metal element under different conditions was investigated. The conditions were sulfuric acid concentration (1.5, 2.0, 2.5, 3.0, and 3.5 mol·L^{-1}), oxalic acid concentration (10, 15, 20, 25, and 30 g·L^{-1}), liquid-to-solid ratio (6, 8, 10, 12, and 14 mL·g^{-1}), reaction temperature (40, 55, 70, 85, and 100 °C) and reaction time (20, 60, 100, 140, and 180 min).

For the accuracy of the experimental results, three parallel experiments were carried out for each group of experiments during the whole leaching process, and the average value was taken as the final result. The formula for the leaching rate of each metal element is shown in Equation (1):

$$\alpha = \frac{cv}{m\omega} \times 100\% \quad (1)$$

where α is the leaching rate of each metal (%); c is the content of each metal in the leaching solution ($g \cdot L^{-1}$); v is the volume of leaching solution (L); m is the mass of cathode powder (g); ω is the content of each metal element in the cathode powder (%).

2.3. Characterization of Samples

An inductively coupled plasma atomic emission spectrometer (Agilent ICP-OES730, Palo Alto, CA, America) was used to determine the concentration of metal elements in the spent cathode powder and its leaching solution. X-ray photoelectron spectroscopy (Thermo ESCALAB 250Xi, Waltham, MA, America) was used to analyze the valence of metal elements on the surface of cathode powder. An X-ray powder diffractometer (BRUCKER D8 ADVANCE, Billerica, MA, America) was used to analyze the phase of the cathode powder and its residue. The morphology and distribution of valuable metal elements of spent cathode materials before and after leaching were studied by using emission scanning electron microscopy (Hitachi SU8020, Chiyoda, TKY, Japan).

3. Results and Discussion

3.1. Analysis of Original Cathode Powder

ICP-OES was used to measure the concentration of each metal element in the solution after complete leaching with aqua regia, to determine the content of the valuable metals in the sample. The results are shown in Table 2.

Table 2. The content of metal elements in spent lithium-ion batteries cathode material.

Metal Element	Li	Ni	Co	Mn	Fe	Al	Others
Content (wt%)	6.87	41.13	5.05	4.71	0.21	0.28	trace

As can be seen from Table 2, the molar ratio of nickel, cobalt, and manganese in the cathode material is close to 8:1:1. It was preliminarily speculated that this batch of spent battery samples belongs to the NCM811 lithium-ion battery.

XPS was used to analyze the valence state of each metal in the original spent ternary cathode material, as shown in Figure 1. It shows only Ni^{2+} indicating NiO as the nickel species. Additionally, cobalt has valences of +2 and +3. However, manganese coexists as Mn^{2+}, Mn^{3+}, and Mn^{4+}. The high-priced Co^{3+}, Mn^{3+}, and Mn^{4+} are insoluble and difficult to be leached, so it is usually necessary to use reducing agents to reduce them to improve the metal leaching rate.

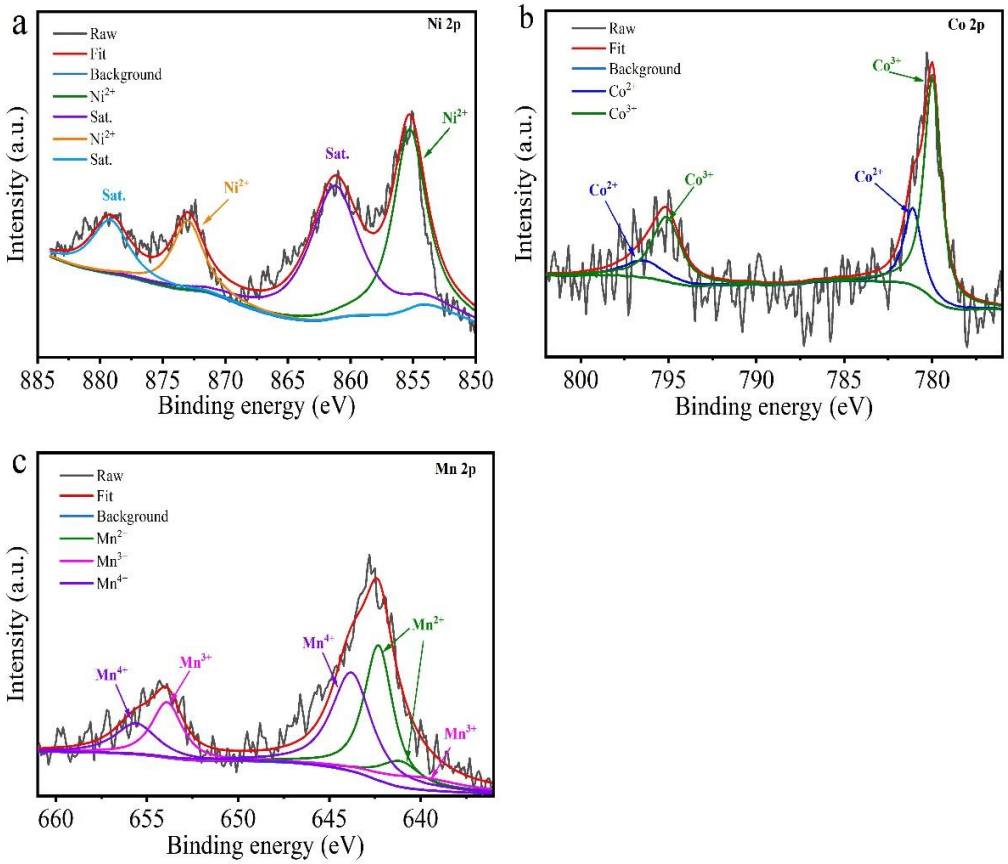


Figure 1. The XPS of original cathode powder. (**a**) the valence state of Ni. (**b**) the valence state of Co. (**c**) the valence state of Mn.

In this experiment, oxalic acid was used as reducing agent to leach spent ternary cathode materials of lithium-ion batteries in sulfuric acid solution, and the reaction was as follows:

$$LiNi_{0.8}Co_{0.1}Mn_{0.1}O_2 + H_2SO_4 + H_2C_2O_4 \rightarrow Li_2SO_4 + NiSO_4 + CoSO_4 + MnSO_4 + H_2O + CO_2 \uparrow \quad (2)$$

3.2. Leaching Conditions

3.2.1. The Effect of Sulfuric Acid Concentration on Leaching Rate

Figure 2a shows the influence of sulfuric acid concentration on the metal leaching rate under the conditions of oxalic acid concentration at 15 g·L^{-1}, liquid-to-solid ratio at 8 mL·g^{-1}, reaction temperature at 85 °C, and reaction time at 60 min. The leaching rate of the four metals firstly increased and then tended to be stable with the increase in sulfuric acid concentration. In the process of sulfuric acid concentration increasing from 1.5 mol·L^{-1} to 2.5 mol·L^{-1}, the metal leaching rate curve showed a rapid rise stage. The leaching rate of Li increased from 59.83% to 83.25%, the leaching rate of Ni increased from 55.41% to 77.36%, the leaching rate of Co increased from 50.45% to 67.42%, and the leaching rate of Mn increased from 53.23% to 69.63%. The concentration of sulfuric acid continued to increase to 3.5 mol·L^{-1}, the leaching rate of each metal did not increase obviously, but nearly remained stable. It can also be seen that the leaching rate of Li was much higher than that of the other three metal ions, because the binding energy of the Li–O bond is the weakest in the crystal structure of cathode material [33], and Li is relatively easy to be leached. Therefore, the sulfuric acid concentration at 2.5 mol·L^{-1} is selected for subsequent experiments.

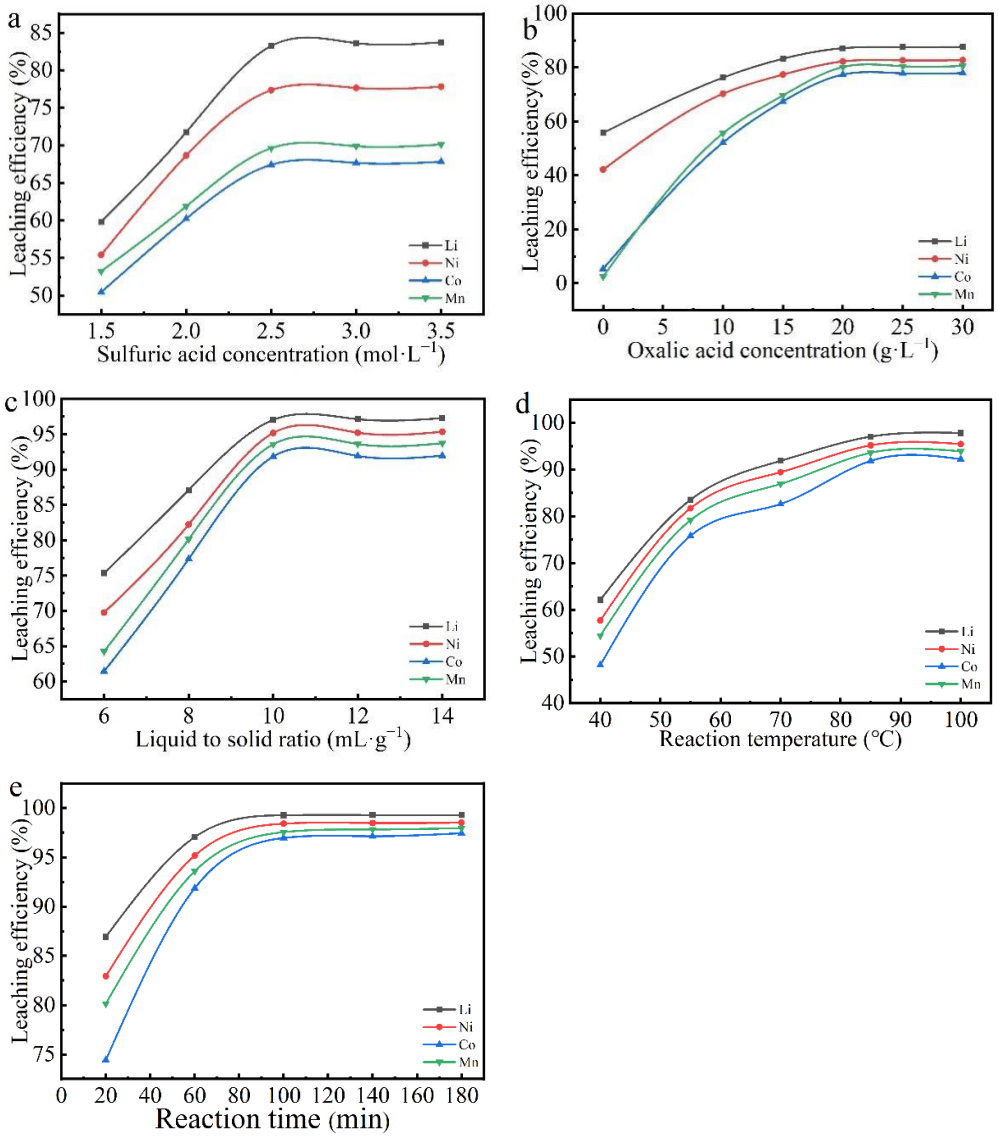


Figure 2. The effect of (**a**) sulfuric acid concentration, (**b**) oxalic acid concentration, (**c**) liquid-to-solid ratio, (**d**) reaction temperature, and (**e**) reaction time on the leaching rate of valuable metals.

3.2.2. The Effect of Oxalic Acid Concentration on Leaching Rate

Under the conditions of sulfuric acid concentration at 2.5 mol·L^{-1}, liquid-to-solid ratio at 8 mL·g^{-1}, reaction temperature at 85 °C, and reaction time at 60 min, the metal leaching rate curve fluctuated with varied oxalic acid concentration is shown in Figure 2b. When the oxalate concentration was 0 g·L^{-1}, the leaching rate of lithium, nickel, cobalt, and manganese was 55.76%, 42.15%, 5.34%, and 2.48%, respectively. Cobalt and manganese were almost not dissolved without presence of oxalic acid. With the increase in oxalic acid concentration from 10 g·L^{-1} to 20 g·L^{-1}, the leaching rate of Li, Ni, Co, and Mn increased from 76.24%, 70.25%, 52.17.%, and 55.63% to 87.12%, 82.23%, 77.35%, and 80.14%. When the concentration of oxalic acid increased to 30 g·L^{-1}, the leaching rate of each metal ion did not change a lot, and almost formed a plateau. The results show that the addition of oxalic acid significantly increases the leaching rate of Co and Mn, indicating that oxalic acid has a good reduction effect on Co^{3+}, Mn^{3+}, and Mn^{4+}, and the higher the concentration of oxalic acid, the higher the leaching rate. The leaching rate of Li and Ni increased with the increase in oxalic acid concentration to a certain extent, because the crystal structure of cathode material is destroyed after the destruction of the Co–O bond and Mn–O bond

by the leaching agent, then Li and Ni are more easily leached. Therefore, the oxalic acid concentration at 20 $g \cdot L^{-1}$ is chosen as the optimal condition.

3.2.3. The Effect of Liquid-to-Solid Ratio on Leaching Rate

Under the conditions of sulfuric acid concentration at 2.5 $mol \cdot L^{-1}$, oxalic acid concentration at 20 $g \cdot L^{-1}$, reaction temperature at 85 °C, and reaction time at 60 min, the effect of liquid-to-solid ratio on the leaching rate of four metal ions is shown in Figure 2c. It can be seen that the change in leaching rate was divided into two stages: when the liquid-to-solid ratio increased from 6 $mL \cdot g^{-1}$ to 10 $mL \cdot g^{-1}$, the leaching rate of each metal ion increased almost linearly. When the liquid-to-solid ratio at 10 $mL \cdot g^{-1}$, the leaching rate of Li, Ni, Co, and Mn reached 97.05%, 95.18%, 91.86%, and 93.58%. When the liquid-to-solid ratio increased from 10 $mL \cdot g^{-1}$ to 14 $mL \cdot g^{-1}$, the leaching rate curve of each metal ion tended to be stable, and the leaching rate did not increase much. When the liquid-to-solid ratio is lower than 10 $mL \cdot g^{-1}$, the viscosity of the solution is large, which is not conducive to the reaction; because the concentration of sulfuric acid and oxalic acid is firm, and the amount of leachate is limited, so the leaching rate of each metal element is low. When the liquid-to-solid ratio is higher than 10 $mL \cdot g^{-1}$, the leaching rate of metal ions is not greatly improved, and the leaching agent is wasted at the same time. Considering that the increase in the concentration of the leaching solution is beneficial to the subsequent recovery of valuable metals, the optimal liquid-to-solid ratio is determined to be 10 $mL \cdot g^{-1}$.

3.2.4. The Effect of Reaction Temperature on Leaching Rate

Figure 2d shows the effect of reaction temperature on the leaching rate of the spent cathode powder. Other conditions were the concentration of sulfuric acid at 2.5 $mol \cdot L^{-1}$, the concentration of oxalic acid at 20 $g \cdot L^{-1}$, the liquid-to-solid ratio at 10 $mL \cdot g^{-1}$, and the reaction time at 60 min. The results show that the leaching rate of each metal in the spent cathode powder increases with the increase in the reaction temperature. As the reaction temperature increased from 40 °C to 85 °C, the leaching rate of Li, Ni, Co, and Mn increased sharply from 62.11%, 57.71%, 48.16%, and 54.46% to 97.05%, 95.18%, 91.86%, and 93.58%. When the reaction temperature increased to 100 °C, the leaching rate changed little, and the leaching rate of Li, Ni, Co, and Mn only increased, respectively, by 0.75%, 0.29%, 0.58%, and 0.32%. The reason why the leaching rate of each metal is affected by temperature is that the leaching reaction of the cathode material is endothermic, and the increase in temperature can improve the feasibility and reaction rate of the reaction. At the same time, the increase in temperature can intensify the movement of particles, which is beneficial to the mass transfer process of the reaction, thereby increasing the leaching rate. Considering that after the reaction temperature exceeded 85 °C, the leaching rate of each metal was limited, and high temperature has higher requirements on equipment and increases energy consumption, the optimal reaction temperature is 85 °C.

3.2.5. The Effect of Reaction Time on Leaching Rate

The effect of reaction time on the leaching rate of each metal is shown in Figure 2e. The sulfuric acid concentration at 2.5 $mol \cdot L^{-1}$, the oxalic acid concentration at 20 $g \cdot L^{-1}$, the liquid-to-solid ratio at 10 $mL \cdot g^{-1}$, the reaction temperature at 85 °C was fixed, and the reaction time was varied within the range of 20 min to 180 min. It can be seen that when the reaction time was 20 min, the leaching rate of Li, Ni, Co, and Mn was 49.88%, 41.29%, 31.29%, and 37.65%, respectively. With the prolongation of the reaction time, the leaching rate of each metal increased rapidly and reached the maximum value at 100 min. At this time, the leaching rate of Li, Ni, Co, and Mn was 99.26%, 98.41%, 96.95%, and 97.54%. Then, the reaction time was extended to 180 min, and the leaching rate curve of each metal became stable. This shows that when the reaction time is 100 min, the leaching reaction is close to the limit, and time is no longer the key factor affecting the leaching rate. From the perspective of shortening the production cycle, it is more appropriate to choose a reaction time of 100 min.

3.3. Kinetic Analysis

In order to explore the leaching kinetics and apparent activation energy of valuable metals from spent lithium-ion batteries recovered with sulfuric acid and oxalic acid, five groups of experiments at different reaction temperatures were designed under the experimental conditions of sulfuric acid concentration at 2.5 mol·L^{-1}, oxalic acid concentration at 20 g·L^{-1} and liquid-to-solid ratio at 10 mL·g^{-1}. The leaching temperatures were set at 25 °C, 40 °C, 55 °C, 70 °C, and 85 °C, respectively. The leaching time of each group was set at 20 min, 40 min, 60 min, 80 min, and 100 min. The kinetic curves of the leaching rate for each metal ion at different temperatures with the change in time are recorded, as shown in Figure 3.

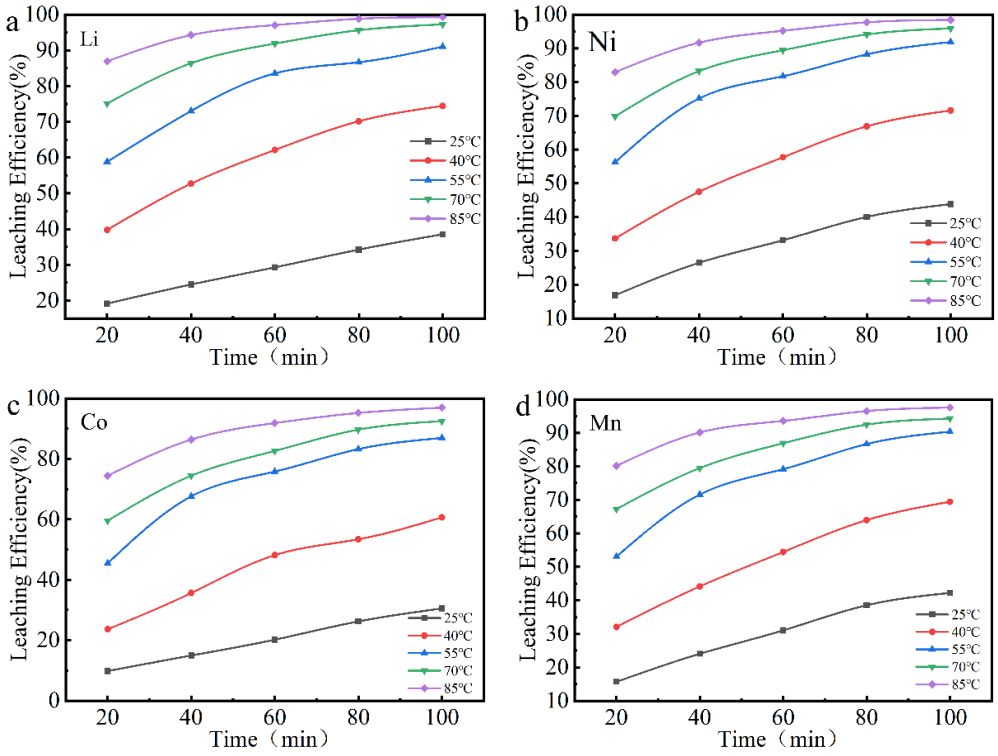


Figure 3. The kinetic curves of leaching rate for each metal ion of spent lithium-ion battery cathode powder: (**a**) Li, (**b**) Ni, (**c**) Co, and (**d**) Mn.

The leaching of spent lithium-ion battery cathode powder belongs to a liquid–solid reaction. With the leaching progression of the cathode material, the product is dissolved in water, and the shape size of the solid particle gradually decreases until it completely is disappeared. This kind of reaction can be described by the "unreacted shrinking core model" [34]. The model can be divided into the following three types: (A) surface chemical control model; (B) diffusion control model; (C) log rate law model [35]. In order to describe the leaching process more accurately, the Avrami model was used to describe the leaching kinetics of the cathode material of lithium-ion batteries. Avrami model was originally used to describe the kinetics of crystal growth in solution. Since the cathode material of the spent battery is continuously dissolved and no solid phase is generated, solid leaching dissolution can be regarded as the reversed process of crystal growth in solution. Therefore, Avrami model is suitable to describe the kinetics of lithium-ion battery leaching [36]. The above four dynamic model equations are as follows:

$$1 - (1 - x)^{1/3} = k_1 t \quad (3)$$

$$1 - 2/3x - (1 - x)^{2/3} = k_2 t \quad (4)$$

$$(-\ln(1 - x))^2 = k_3 t \quad (5)$$

$$\ln[-\ln(1-x)] = \ln k_4 + n \ln t \quad (6)$$

In the above formula, x is the leaching rate of each metal ion (%); k_1, k_2, k_3, and k_4 represent the different reaction rate constant (min^{-1}); t is reaction time (min); n is the order of the reaction.

The above four kinetic models were used to fit the leaching kinetic data of each metal. Since the leaching kinetic curves of Li, Ni, Co, and Mn are the same, the fitting results of the four leaching kinetic models by Co are represented and selected. The corresponding correlation coefficient R^2 between each model and Co kinetic data is shown in Table 3.

Table 3. The fitting results of four kinetic models for Co leaching.

T/°C	Surface Chemical Control Model	Diffusion Control Model	Log Rate Law Model	Avrami Model
25	0.9680	0.9247	0.9263	0.9915
40	0.9563	0.9622	0.9528	0.9954
55	0.9117	0.9329	0.9653	0.9928
70	0.9558	0.9605	0.9340	0.9946
85	0.9444	0.9406	0.9641	0.9985

When the three models of the unreacted shrinking core model were used to describe the leaching process of Co, some relevant data points were scattered, the correlation coefficient R^2 was small, and the correlation fitting was poor. Therefore, the unreacted shrinking core model was not suitable to describe the leaching of Li, Ni, Co, and Mn. When the Avrami model was used to describe the Co leaching process, the correlation coefficients were all greater than 0.99, showing a good fitting effect. The fitting results of the Avrami model to the kinetic data of four metals are shown in Figure 4.

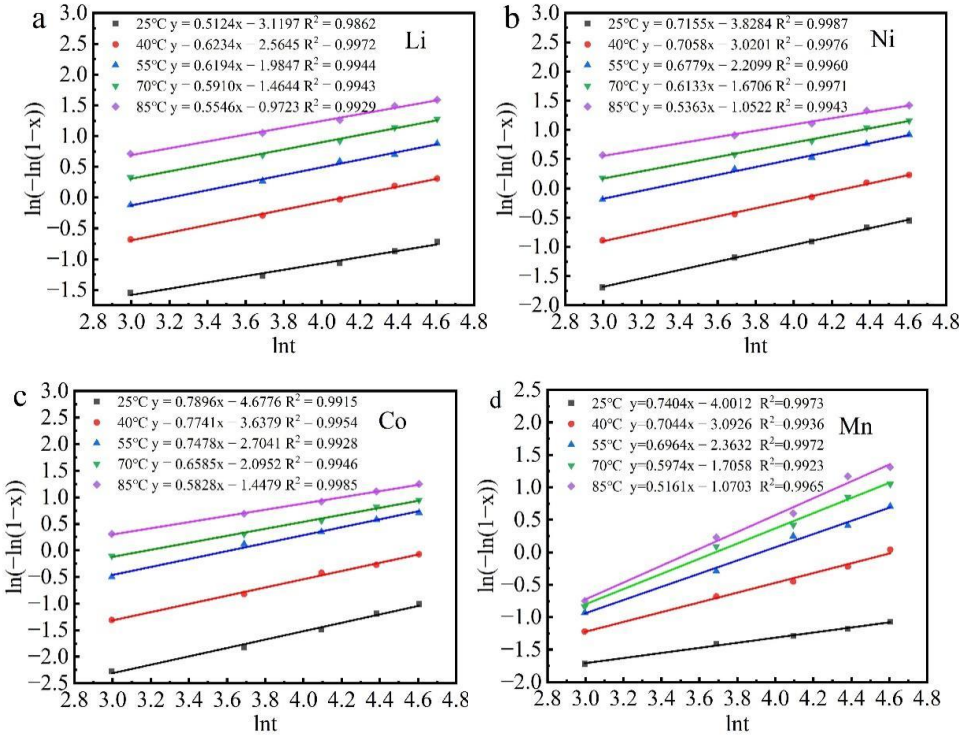


Figure 4. The fitting results of the Avrami model to the kinetic data of four metals: (**a**) Li, (**b**) Ni, (**c**) Co, and (**d**) Mn.

As can be seen from the Figure 4, the fitting coefficients of the four metal elements at different temperatures were all greater than 0.98, indicating that the Avrami equation model can well reflect the whole leaching process. It is generally believed that when the

parameter n in Avrami model is greater than 0.5, leaching is controlled by surface chemical reaction. When n is less than 0.5, leaching is controlled by diffusion [37]. The n values of the four metals at different temperatures were all greater than 0.5, and it was preliminarily concluded that the surface chemical reaction was the control of the four metals' leaching process. The $\ln k$ values of the fitted curves of Li, Ni, Co, and Mn all increased with the increase in temperature, indicating that temperature could significantly change the rate of leaching reaction.

The Arrhenius equation was used to calculate the apparent activation energy of four metals in order to clarify the control steps of the leaching process [38].

$$k = Ae^{-Ea/RT} \tag{7}$$

where k is the reaction rate constant (min^{-1}); A is the frequency factor (min^{-1}); Ea is the apparent activation energy ($kJ \cdot mol^{-1}$); R is the gas constant (R = 8.314 $J \cdot K^{-1} \cdot mol^{-1}$); T is the absolute temperature (K).

The Arrhenius formula is fitted with different $\ln k$ values from 25 to 85 °C as the ordinate and 1000/T as the abscissa, and the result is shown in Figure 5. The slopes of the fitted curves for Li, Ni, Co, and Mn are −3.8441, −4.9321, −5.7222, and −5.1659. The apparent activation energy can be obtained by combining the slope with the gas constant R. The activation energies of Li, Ni, Co, and Mn were 31.96 $kJ \cdot mol^{-1}$, 41.01 $kJ \cdot mol^{-1}$, 47.57 $kJ \cdot mol^{-1}$ and 42.95 $kJ \cdot mol^{-1}$, respectively. The activation energy of Li is less than 40 $kJ \cdot mol^{-1}$, indicating that diffusion is the control step of the Li leaching process. The activation energies of the other three elements are all greater than 40 $kJ \cdot mol^{-1}$, and the higher activation energies indicate that the control of the leaching process of these metals is the surface chemical reaction [39]. From the perspective of activation energy, the higher the activation energy for the leaching reaction, the more difficult the leaching reaction is. Therefore, in the process of leaching spent cathode materials, Li is easiest to be leached, while Co is the most difficult to be leached, which is also consistent with the above single factor experiment results.

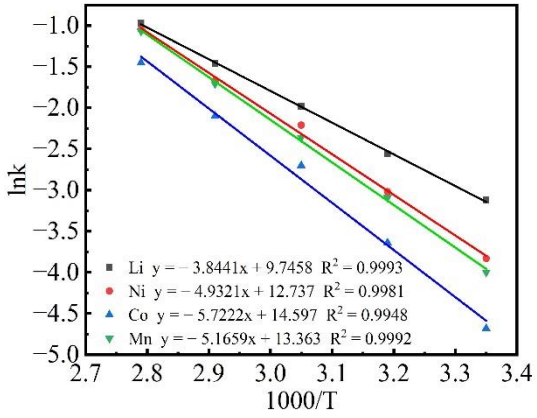


Figure 5. Arrhenius plots for the leaching of Li, Ni, Co, and Mn.

3.4. Characterization of Spent Lithium-Ion Cathode Powder before and after Leaching

3.4.1. XRD Analysis

In order to determine the change in phase in the leaching process of cathode powder, XRD was used to detect and analyze the original spent lithium-ion battery solid powder and its leaching residue, and the results are shown in Figure 6. The XRD pattern of the original spent lithium-ion battery powder shows good characteristic peaks of $LiNi_{0.8}Co_{0.1}Mn_{0.1}O_2$, and no diffraction peaks of other substances are detected. As can be seen from the XRD pattern of leaching residue, part of the diffraction peaks of $LiNi_{0.8}Co_{0.1}Mn_{0.1}O_2$ after leaching split, and most of the diffraction peaks decrease in intensity and disappear. This indicates that the crystal structure of $LiNi_{0.8}Co_{0.1}Mn_{0.1}O_2$ was destroyed and almost completely

leached during the leaching process. In addition, the XRD pattern of leaching residue shows the diffraction peak of C, which is not shown in the XRD pattern of the original battery powder. This is because the content of C in the original spent lithium-ion battery powder is low, which is below the limit of detection, so the diffraction peak of C cannot be shown on the XRD pattern. After leaching, the solid residue becomes less and the relative content of C becomes higher, so there is an obvious diffraction peak of C in the XRD pattern of the leached residue.

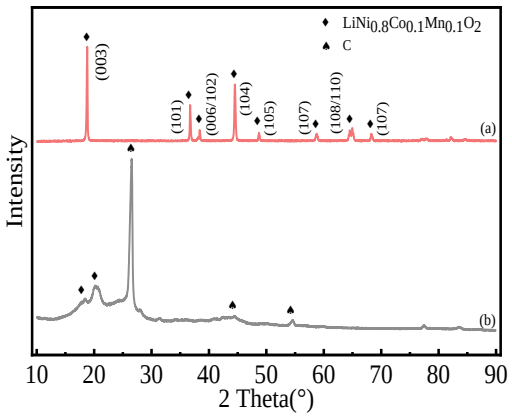


Figure 6. The XRD pattern of cathode powder before and after leaching: (**a**) the cathode powder before leaching, and (**b**) the cathode powder after leaching.

3.4.2. SEM-EDS Analysis

For purpose of studying the microstructure and chemical composition of spent ternary lithium-ion battery cathode powder before and after leaching, SEM-EDS was used to characterize and analyze it. As shown in Figure 7a, the appearance of the particles before leaching is spherical with different particle sizes, and Ni, Co, and Mn are uniformly distributed in the spherical particles. Because the energy of Li produced by the X-ray strafing is small, so Li cannot be detected and analyzed. On account of the corrosion behavior of the leaching agent, Figure 7b shows that the particles after leaching are completely irregular and spongy. This indicates that the leaching of cathode powder is an irregular corrosion reduction process rather than a uniform shrinking process, which again proves that the leaching process is inconsistent with the assumption of the unreacted shrinking core model. After the leaching process, three metal elements disappear in vast numbers, and the remaining valuable metals are unevenly dispersed in the residue. The content of nickel, cobalt, and manganese can be calculated from the intensity of the peaks and the response value of this element according to the spectrum of mapping. The peaks at 0–2 Kev, show an obvious decrease after leaching, along with peaks at 6–9 Kev disappeared at the same response value. Therefore, the content of nickel, cobalt, and manganese in the residue is lower. This is consistent with the above experimental results and XRD analysis results. However, the specific content of the valuable metal is subject to ICP-OES results.

a

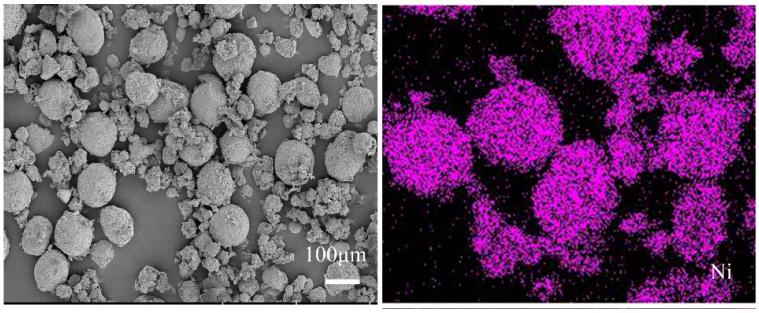


Figure 7. *Cont.*

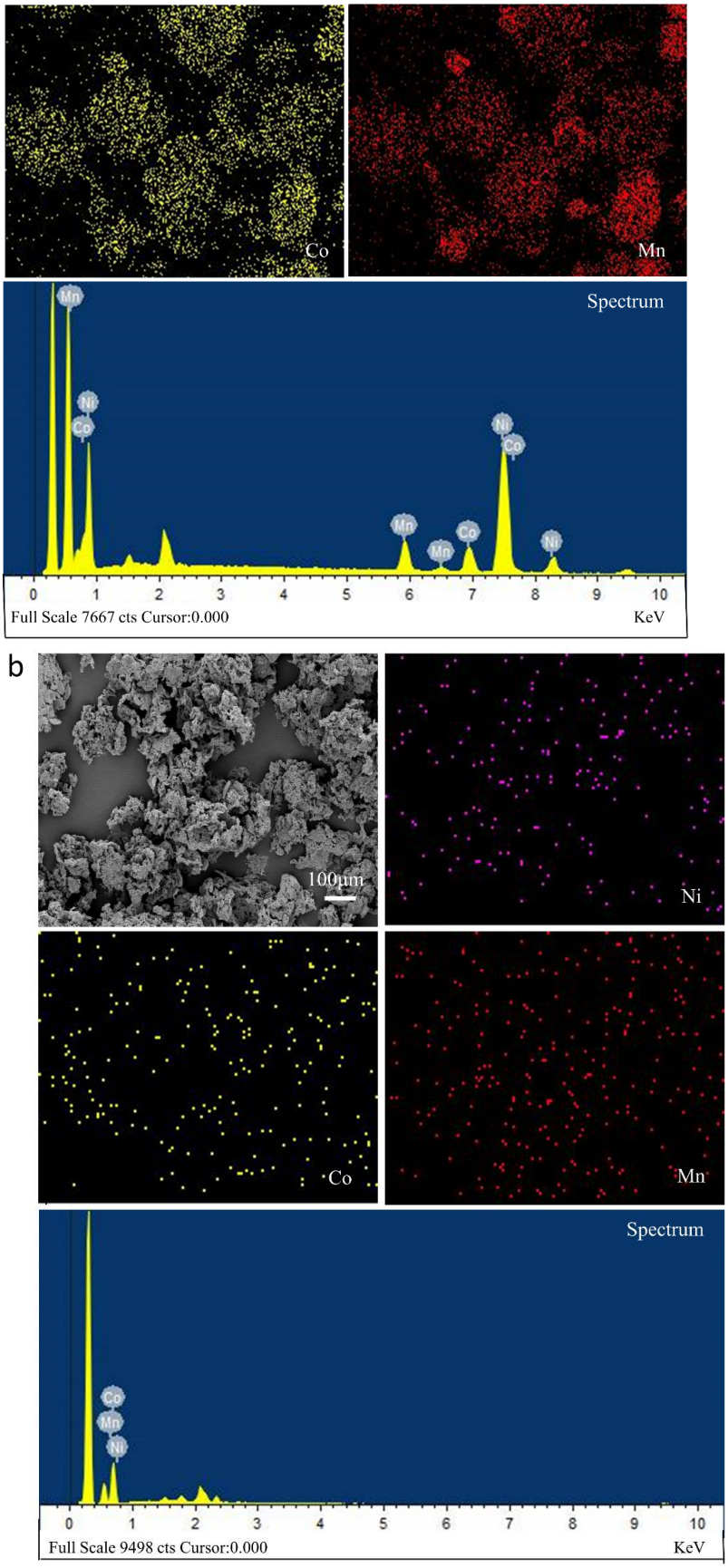


Figure 7. The SEM-EDS images of cathode powder before and after leaching: (**a**) the cathode powder before leaching, and (**b**) the cathode powder after leaching.

4. Conclusions

With the synergistic effect of the reducing ability of oxalic acid and the acidic strength of sulfuric acid, this study proposes a method for recovering valuable metals from spent lithium-ion battery cathode materials with composite leaching agents of sulfuric acid and oxalic acid. The following conclusions are drawn from the leaching experimental results and characterization analysis. Under the optimized conditions of sulfuric acid concentration at 2.5 mol·L^{-1}, oxalic acid concentration at 20 g·L^{-1}, liquid-to-solid ratio at 10 mL·g^{-1}, reaction temperature at 85 °C, and reaction time at 100 min, the leaching rate of Li, Ni, Co, and Mn was, respectively, 99.26%, 98.41%, 96.95%, and 97.54%. At the same time, the characterizations of XRD and SEM-EDS further validated that the valuable metals have been almost completely leached. By fitting four kinds of kinetic models, the leaching kinetics of Li, Ni, Co, and Mn were determined to conform to the Avrami model, and their activation energies were 31.96 kJ·mol^{-1}, 41.01 kJ·mol^{-1}, 47.57 kJ·mol^{-1}, and 42.95 kJ·mol^{-1}. Additionally, the diffusion was the control of the Li leaching process, and the surface chemical reaction was the control of the other three metals. The process of recovering valuable metals from spent lithium-ion batteries with composite leaching agents of sulfuric acid and oxalic acid has the advantages of low environmental pollution, low production cost, and high recovery rate, which has a certain guiding significance for industrial production.

Author Contributions: Conceptualization, C.Y. and H.W.; methodology, C.Y. and J.W.; software, C.Y.; validation, H.W. and J.W.; formal analysis, C.Y.; investigation, Y.H.; resources, S.W.; data curation, P.Y. and P.Z.; writing—original draft preparation, C.Y.; writing—review and editing, J.W.; visualization, C.Y.; supervision, J.W.; project administration, H.W. and J.W.; funding acquisition, H.W. All authors have read and agreed to the published version of the manuscript.

Funding: The funding supports for this study were obtained from the National Natural Science Foundation of China (51864012); the Key Projects Supported by Science and Technology in Guizhou Province ([2022]key020); the Major Special Projects in Guizhou Province ([2022]003); Guizhou Provincial Science and Technology Plan Project ([2016]5302, [2017]5788, [2018]5781, [2019]1411, [2019]2841), Tongren Science and Technology Plan Project ([2021]13). The authors sincerely thank the reviewers for their views and suggestions to further improve the quality of the manuscript.

Conflicts of Interest: The authors declare no conflict of interest.

References

1. Kim, T.; Song, W.; Son, D.-Y.; Ono, L.K.; Qi, Y. Lithium-ion batteries: Outlook on present, future, and hybridized technologies. *J. Mater. Chem. A* **2019**, *7*, 2942–2964. [CrossRef]
2. Tang, J.; Wu, F.; Dai, X.; Zhou, J.; Pang, H.; Duan, X.; Xiao, B.; Li, D.; Long, J. Robust MXene adding enables the stable interface of silicon anodes for high-performance Li-ion batteries. *Chem. Eng. J.* **2022**, *452*, 139139. [CrossRef]
3. Gandoman, F.H.; Jaguemont, J.; Goutam, S.; Gopalakrishnan, R.; Firouz, Y.; Kalogiannis, T.; Omar, N.; Van Mierlo, J. Concept of reliability and safety assessment of lithium-ion batteries in electric vehicles: Basics, progress, and challenges. *Appl. Energy* **2019**, *251*, 113343. [CrossRef]
4. Tian, Y.; Zeng, G.; Rutt, A.; Shi, T.; Kim, H.; Wang, J.; Koettgen, J.; Sun, Y.; Ouyang, B.; Chen, T.; et al. Promises and Challenges of Next-Generation "Beyond Li-Ion" Batteries for Electric Vehicles and Grid Decarboniza-tion. *Chem. Rev.* **2020**, *121*, 1623–1669. [CrossRef]
5. Zhao, T.; Yao, Y.; Wang, M.; Chen, R.; Yu, Y.; Wu, F.; Zhang, C. Preparation of MnO_2-Modified Graphite Sorbents from Spent Li-Ion Batteries for the Treatment of Water Contaminated by Lead, Cadmium, and Silver. *Acs. Appl. Mater. Inter.* **2017**, *9*, 25369–25376. [CrossRef]
6. Lin, J.; Li, L.; Fan, E.; Liu, C.; Zhang, X.; Cao, H.; Sun, Z.H.; Chen, R. Conversion Mechanisms of Selective Extraction of Lithium from Spent Lithium-Ion Batteries by Sulfation Roasting. *ACS Appl. Mater. Interfaces* **2020**, *12*, 18482–18489. [CrossRef]
7. Fujita, T.; Chen, H.; Wang, K.-T.; He, C.-L.; Wang, Y.-B.; Dodbiba, G.; Wei, Y.-Z. Reduction, reuse and recycle of spent Li-ion batteries for automobiles: A review. *Int. J. Miner. Met. Mater.* **2021**, *28*, 179–192. [CrossRef]
8. Xia, X.; Li, P. A review of the life cycle assessment of electric vehicles: Considering the influence of batteries. *Sci. Total Environ.* **2022**, *814*, 152870. [CrossRef]
9. Wang, Y.; Xu, Z.; Zhang, X.; Yang, E.; Tu, Y. A green process to recover valuable metals from the spent ternary lithium-ion batteries. *Sep. Purif. Technol.* **2022**, *299*, 121782. [CrossRef]

10. Zhang, G.; Yuan, X.; He, Y.; Wang, H.; Zhang, T.; Xie, W. Recent advances in pretreating technology for recycling valuable metals from spent lithium-ion batteries. *J. Hazard. Mater.* **2021**, *406*, 124332. [CrossRef]
11. Mrozik, W.; Rajaeifar, M.A.; Heidrich, O.; Christensen, P. Environmental impacts, pollution sources and pathways of spent lithium-ion batteries. *Energy Environ. Sci.* **2021**, *14*, 6099–6121. [CrossRef]
12. Ma, Y.; Tang, J.; Wanaldi, R.; Zhou, X.; Wang, H.; Zhou, C.; Yang, J. A promising selective recovery process of valuable metals from spent lithium ion batteries via reduction roasting and ammonia leaching. *J. Hazard. Mater.* **2021**, *402*, 123491. [CrossRef]
13. Tian, G.; Yuan, G.; Aleksandrov, A.; Zhang, T.; Li, Z.; FathollahiFard, A.M.; Ivanov, M. Recycling of Spent Lithium-Ion Bat-teries: A Comprehensive Review for Identification of Main Challenges and Future Research Trends. *Sustain. Energy. Techn.* **2022**, *53*, 102447.
14. Zheng, X.; Zhu, Z.; Lin, X.; Zhang, Y.; He, Y.; Cao, H.; Sun, Z. A Mini-Review on Metal Recycling from Spent Lithium Ion Batteries. *Engineering* **2018**, *4*, 361–370. [CrossRef]
15. Makuza, B.; Tian, Q.; Guo, X.; Chattopadhyay, K.; Yu, D. Pyrometallurgical options for recycling spent lithium-ion batteries: A comprehensive review. *J. Power Sources* **2021**, *491*, 229622. [CrossRef]
16. Roy, J.J.; Cao, B.; Madhavi, S. A review on the recycling of spent lithium-ion batteries (LIBs) by the bioleaching approach. *Chemosphere* **2021**, *282*, 130944. [CrossRef] [PubMed]
17. Horeh, N.B.; Mousavi, S.; Shojaosadati, S. Bioleaching of valuable metals from spent lithium-ion mobile phone batteries using Aspergillus niger. *J. Power Sources* **2016**, *320*, 257–266. [CrossRef]
18. Yao, Y.; Zhu, M.; Zhao, Z.; Tong, B.; Fan, Y.; Hua, Z. Hydrometallurgical Processes for Recycling Spent Lithium-Ion Batteries: A Critical Review. *ACS Sustain. Chem. Eng.* **2018**, *6*, 13611–13627. [CrossRef]
19. Ferreira, D.A.; Prados, L.M.Z.; Majuste, D.; Mansur, M.B. Hydrometallurgical separation of aluminium, cobalt, copper and lithium from spent Li-ion batteries. *J. Power Sources* **2009**, *187*, 238–246. [CrossRef]
20. Li, J.; Li, X.; Hu, Q.; Wang, Z.; Zheng, J.; Wu, L.; Zhang, L. Study of extraction and purification of Ni, Co and Mn from spent battery material. *Hydrometallurgy* **2009**, *99*, 7–12. [CrossRef]
21. Chen, H.; Gu, S.; Guo, Y.; Dai, X.; Zeng, L.; Wang, K.; He, C.; Dodbiba, G.; Wei, Y.; Fujita, T. Leaching of cathode materials from spent lithium-ion batteries by using a mixture of ascorbic acid and HNO3. *Hydrometallurgy* **2021**, *205*, 105746. [CrossRef]
22. Zhao, J.; Zhang, B.; Xie, H.; Qu, J.; Qu, X.; Xing, P.; Yin, H. Hydrometallurgical recovery of spent cobalt-based lithium-ion battery cathodes using ethanol as the reducing agent. *Environ. Res.* **2020**, *181*, 108803. [CrossRef] [PubMed]
23. Xiao, J.; Li, J.; Xu, Z. Challenges to Future Development of Spent Lithium Ion Batteries Recovery from Environmental and Technological Perspectives. *Environ. Sci. Technol.* **2019**, *54*, 9–25. [CrossRef] [PubMed]
24. Chen, X.; Zhou, T. Hydrometallurgical process for the recovery of metal values from spent lithium-ion batteries in citric acid media. *Waste Manag. Res. J. Sustain. Circ. Econ.* **2014**, *32*, 1083–1093. [CrossRef] [PubMed]
25. Li, L.; Fan, E.; Guan, Y.; Zhang, X.; Xue, Q.; Wei, L.; Wu, F.; Chen, R. Sustainable Recovery of Cathode Materials from Spent Lithium-Ion Batteries Using Lactic Acid Leaching System. *ACS Sustain. Chem. Eng.* **2017**, *5*, 5224–5233. [CrossRef]
26. Shi, P. The Study of Recovery Technology of Ternary Cathode Materials from Spent Lithium-Ion Batteries. Master's Thesis, Beijing Institute of Technology, Beijing, China, 2015.
27. Meshram, P.; Mishra, A.; Sahu, R. Environmental impact of spent lithium ion batteries and green recycling perspectives by organic acids—A review. *Chemosphere* **2020**, *242*, 125291. [CrossRef]
28. Fan, X.; Song, C.; Lu, X.; Shi, Y.; Yang, S.; Zheng, F.; Huang, Y.; Liu, K.; Wang, H.; Li, Q. Separation and Recovery of Valuable Metals from Spent Lithium-Ion Batteries via Concentrated Sulfuric Acid Leaching and Regeneration of $LiNi_{1/3}Co_{1/3}Mn_{1/3}O_2$. *J. Alloys Compd.* **2021**, *863*, 158775. [CrossRef]
29. Li, L.; Lu, J.; Zhai, L.; Zhang, X.; Curtiss, L.; Jin, Y.; Wu, F.; Chen, R.; Amine, K.; China Electric Power Research Institute; et al. A facile recovery process for cathodes from spent lithium iron phosphate batteries by using oxalic acid. *CSEE J. Power Energy Syst.* **2018**, *4*, 219–225. [CrossRef]
30. Wu, W.; Wang, C.; Bao, W.; Li, H. Selective Reduction Leaching of Vanadium and Iron by Oxalic Acid from Spent V_2O_5-WO_3/TiO_2 Catalyst. *Hydrometallurgy* **2018**, *179*, 52–59. [CrossRef]
31. Maddah, F.; Alitabar, M.; Yoozbashizadeh, H. Reductive leaching of indium from the neutral leaching residue using oxalic acid in sulfuric acid solution. *Int. J. Miner. Met. Mater.* **2021**, *28*, 373–379. [CrossRef]
32. Wang, Y.; Liu, B.; Sun, H.; Huang, Y.; Han, G. Selective extraction and recovery of tin from hazardous zinc-leaching residue by oxalic acid/sulfuric acid mixture leaching and hydrolytic precipitation. *J. Clean. Prod.* **2022**, *342*, 130955. [CrossRef]
33. Binder, J.O.; Culver, S.P.; Zeier, W.G.; Janek, J. A Rapid and Facile Approach for the Recycling of High-Performance $LiNi_{1-x-y}Co_xMn_yO_2$ Active Materials. *ChemSusChem* **2021**, *14*, 441–448. [CrossRef] [PubMed]
34. Chen, G.; Jiang, C.; Liu, R.; Xie, Z.; Liu, Z.; Cen, S.; Tao, C.; Guo, S. Leaching kinetics of manganese from pyrolusite using pyrite as a reductant under microwave heating. *Sep. Purif. Technol.* **2021**, *277*, 119472. [CrossRef]
35. Zhu, B.; Zhang, Y.; Zou, Y.; Yang, Z.; Zhang, B.; Zhao, Y.; Zhang, M.; Meng, Q.; Dong, P. Leaching kinetics and interface reaction of $LiNi_{0.6}Co_{0.2}Mn_{0.2}O_2$ materials from spent LIBs using GKB as reductant. *J. Environ. Manag.* **2021**, *300*, 113710. [CrossRef] [PubMed]
36. Meng, F.; Liu, Q.; Kim, R.; Wang, J.; Liu, G.; Ghahreman, A. Selective recovery of valuable metals from industrial waste lithium-ion batteries using citric acid under reductive conditions: Leaching optimization and kinetic analysis. *Hydrometallurgy* **2020**, *191*, 105160. [CrossRef]

37. George, R.; Sugunan, S. Kinetics of adsorption of lipase onto different mesoporous materials: Evaluation of Avrami model and leaching studies. *J. Mol. Catal. B Enzym.* **2014**, *105*, 26–32. [CrossRef]
38. Ebrahimzade, H.; Khayati, G.R.; Schaffie, M. Leaching kinetics of valuable metals from waste Li-ion batteries using neural network approach. *J. Mater. Cycles Waste Manag.* **2018**, *20*, 2117–2129. [CrossRef]
39. Ajiboye, E.A.; Panda, P.K.; Adebayo, A.O.; Ajayi, O.O.; Tripathy, B.C.; Ghosh, M.K.; Basu, S. Leaching Kinetics of Cu, Ni and Zn from Waste Silica Rich Integrated Circuits Using Mild Nitric Acid. *Hydrometallurgy* **2019**, *188*, 161–168. [CrossRef]